Journal of Sustainable Construction Materials and Technologies

Manuscript 1185

Development of a Self-Cured Alkali-Activated Mortar

Kübra Ekiz Barış

Follow this and additional works at: https://commons.yildiz.edu.tr/jscmt

 Part of the Biomaterials Commons, Chemical Engineering Commons, Civil and Environmental Engineering Commons, Engineering Science and Materials Commons, Materials Science and Engineering Commons, Mechanical Engineering Commons, and the Molecular, Cellular, and Tissue Engineering Commons

JOURNAL OF SUSTAINABLE CONSTRUCTION MATERIALS AND TECHNOLOGIES 2025;10:263–279

Scan the QR to view
the full-text article on
the journal website

RESEARCH ARTICLE

Development of a Self-Cured Alkali-Activated Mortar

Kübra Ekiz Barış

Department of Architecture, Faculty of Architecture and Design, Kocaeli University, 41300 Kocaeli, Türkiye

ABSTRACT

Alkali-activated mortars (AAM) can be produced with self-curing (SC), which supplies internal moisture to accelerate alkaline-activation reactions. The aim of using SC is to make AAMs with an early-age strength without any additional curing energy consumption and higher CO_2 emissions, and to obtain *in-situ* practical advantages that enable the large-scale application of AAMs. The previous study produced natural pozzolan-based AAMs by applying energy-intensive heat (HC), microwave (MWC), and hybrid (HC + MWC) curing. This study investigates alternative curing regimes that reduce production energy without compromising material properties. The impacts of air curing (AC), water curing (WC), and SC on the properties were investigated. PEG 400 was used as an SC agent. The key findings of the research can be summarized as follows: AC and SC were determined as alternative methods, whereas WC didn't show a positive effect on the properties at either early or later periods. Increasing the curing period from 7 to 90 days greatly improves the properties. However, this increasing rate after 90 days was lower than in the early period. The properties after 28-day AC and SC met the values of HC and MWC. The highest compressive strength (19.20 MPa), flexural strength (3.35 MPa), ultrasound velocity (2.67 km/s), and unit weight (2.26 g/cm^3) were obtained after 365-day SC.

Keywords: Alternative curing regime, Self-curing, Low production energy, Alkali-activated mortar, Curing period

1. Introduction

Curing regimes are essential to AAMs' physical, mechanical, and durability characteristics and microstructures. Various curing regimes in ambient or temperature-controlled environments are generally applied to AAMs and include unsealed ambient, sealed, heating, immersion in water, steam curing, and microwave curing [1]. An inappropriate curing regime may lead to marked physical, mechanical, and durability problems, including low mechanical strengths, freeze-thaw resistance, high porosity, water absorption, shrinkage, and increased efflorescence tendency [2–4].

AC is commonly conducted at ambient temperatures between 20°C and 30°C and relative humidity (RH) of 40–95%. This curing regime is similar to the curing condition of traditional ordinary Portland cement (OPC)-based materials conducted on-site, is more economical because it does not require additional heating and the associated costs, and is applicable, all of which are advantageous in large-scale construction [1]. However, low calcium-containing aluminosilicate precursors, including metakaolin, class F fly ash, volcanic tuff, and volcanic ash, do not completely harden in the first few days after synthesis under ambient temperatures [5, 6]. This restricts the application of these materials in the construction industry [7]. To improve the setting and strength properties of low calcium-based AAMs at earlier ages after production, either the application of thermal curing or the addition of calcium-rich supplementary materials, such as granulated blast furnace slag, OPC, high-calcium fly ash, and gypsum, is necessary. In contrast, high calcium-containing precursors do not require long periods and high temperatures to acquire adequate properties, due to the similarity in their hydration kinetics to OPC [8].

Received 20 April 2025; revised 14 May 2025; accepted 21 May 2025.
Available online 30 June 2025

E-mail address: kubra.ekizbaris@kocaeli.edu.tr (K. E. Barış).

https://doi.org/10.29187/2458-973X.1185
2458-973X/© 2025 Published by Yıldız Technical University Press, İstanbul, Türkiye. This is an open access article under the CC BY-NC 4.0 Licence (https://creativecommons.org/licenses/by-nc/4.0/).

Using heat fluxes from the top and bottom of a heater, HC raises the temperature progressively until it has reached the desired level. The curing period is controlled by an electronic timer of the oven [9]. AAMs are most commonly cured by an HC regime between 60°C and 90°C for 24 to 48 hours [6]. When temperature increases, the energy of molecules increases, which means that heat acts as an accelerator for the development of chemical reactions [10]. Therefore, AAMs acquire most of their strength in the initial hours [11, 12]. However, longer curing periods under elevated temperatures may lead to rapid moisture loss, which causes a decrease in the properties [11], an increase in autogenous and drying shrinkage of AAMs, and the production of a porous microstructure and cracks in the AAMs [13]. To reduce the evaporation rate and prevent extensive moisture loss, sealed curing using wet burlap or plastic (often polyethylene) coverings can be applied [1]. HC leads to greater costs for AAMs and more energy consumption than AC, which may reverse the positive effect of reducing CO_2 emissions produced by AAMs. In addition, large-scale applications are prevented by *in situ* practical challenges when using HC.

Immersing AAMs conduct WC in a water tank at 20–25°C or 65–95°C. In low calcium-containing AAMs, WC leads to dilution of the reaction medium, leaching of the alkaline activators, and decreased mechanical properties [1]. In contrast, in high calcium-containing AAMs, WC leads to lower permeability and water absorption, as well as higher strength and durability characteristics [14], because of the formation of calcium aluminosilicate hydrate (C-A-S-H) gel in the microstructure of the high calcium-based matrix that is produced through the consumption of water [15].

Steam curing involves exposing the AAMs to atmospheric or higher-pressure water vapor. The general temperature range for this curing method is between 70°C and 100°C. This curing regime is frequently applied where a substantially increased early-age strength and early removal of formwork is required, such as in the production of precast concrete elements [16]. According to an experimental study by Huang et al. [17], the compressive strength of bottom ash incorporated slag-based AAMs at an early age was 26% higher after steam curing and 12% lower after WC than that of AC-cured counterparts.

Being a volumetric curing regime, MWC uses electromagnetic radiation with a frequency higher than 1 GHz and a wavelength of less than 10^3 mm [18]. Microwaves generate heat rapidly by using electromagnetic energy that creates internal vibrations at the molecular level. They are therefore appropriate for prefabrication [19]. The use of MWC was a significant advance addressing the primary drawback of HC, which might need a curing period as short as a few seconds [20]. For instance, 120 minutes of MWC equals 48 hours of HC at 75°C [21]. The fly ash-based AAMs had adequate early age strength after MWC at 200 W microwave power in only 60 minutes [22]. In another study, increasing microwave power to 350 W decreased the curing period of fly ash-based AAMs by as much as five minutes [23]. The combination of HC and MWC, which is known as a hybrid curing method, can be applied to reduce the required microwave power and HC period. The fly ash-based AAMs having a compressive strength of over 40 MPa at seven days were produced by applying MWC at 90 W for five minutes, followed by HC at 65 °C for 12 hours [24]. Results from a different study showed that the HC period (24 hours at 80°C) of metakaolin-based AAMs was reduced by two-thirds when MWC (160 W for 12 minutes) was applied after HC [25].

An AC regime leads to lower mechanical properties during early-age curing, especially for low calcium-based AAMs. In contrast, HC, steam, and MWC regimes are associated with higher energy consumption, higher CO_2 emissions, and *in situ* practical issues that prevent the large-scale application of AAMs. Thus, adopting the "self-curing (SC)" regime, which focuses on using chemical additives in the mixture of AAMs, may overcome these obstacles. A SC regime depends on the supply of internal moisture to accelerate the hydration or alkaline activation process and enhance the properties of materials based on cement or AAM 26, 27. The SC agents in this regime reduce water evaporation from the material, increase its moisture retention ability, and prevent cracking during curing [28]. Applying this method is especially beneficial in hot and dry climates because water scarcity can adversely affect the material's early-age strength development. SC enables immediate high strength within 2–3 days. Applying this method also has several advantages, including reduced autogenous and drying shrinkage, enhanced durability, improved fracture resistance, and preservation of reinforcement. SC may also serve as a potential alternative for inadequate curing conditions. Furthermore, the amount of wastewater produced annually in the construction industry may be significantly reduced by applying SC, contributing to sustainability in water management [29].

Various types of chemical additives, such as calcium hydroxide, gypsum, nano SiO_2, nano Al_2O_3, silica fume, synthetic resins, polyvalent alcohol, xylitol, polyoxyethylene, sorbitol, glycerin, sodium pyrrolidone carboxylate, phytosterols, hyaluronic acid, acetyl alcohol, or polyacrylic acid, stearyl alcohol, polyethylene glycol, butylene glycol, propylene

glycol, and neopentyl glycol may be used for the production of cement-based or AAMs. The optimum percentage of these additives is between 0.1 and 5 wt% of the cement or aluminosilicate precursor content [30].

The mechanical properties of metakaolin-based AAM increased by adding 5% and 10% calcium hydroxide under the AC conditions at 20°C [31]. High-calcium fly ash's compressive strength improved significantly after adding calcium chloride, calcium sulfate, sodium sulfate, and sucrose at 1% and 2% of fly ash [32]. In another study, to decrease setting time and increase shear strength, nano SiO_2 and nano Al_2O_3 were added in high-calcium fly ash cured with AC [33]. Partial replacement of OPC with low-calcium fly ash accelerated the curing stage of AAM compared to using HC [34]. The addition of acrylic resin emulsion and polyvinyl acetate resin (1%) into the metakaolin/slag-based AAMs resulted in an increase in the mechanical performance after curing at 20°C and 99% RH, for 28 days [35]. The metakaolin-based AAM with 0-3% polyethylene glycol (PEG) incorporation was cured under AC conditions. The 28-day compressive strength of the reference sample was 20.1 MPa, and the flexural strength was 3.7 MPa. In comparison, the compressive and flexural strengths of the sample containing 2% PEG 400 during the same curing period were approximately 37.1 MPa and 7.2 MPa, respectively [28]. In another study, metakaolin-based AAM was incorporated with PEG with a molecular weight ranging between 400 and 20000, and was cured at AC conditions for 28 days. The findings showed that adding 10% PEG 400 resulted in a maximum compressive strength of 23.9 MPa and a maximum flexural strength of 2.9 MPa, 57% and 45% higher than reference AAM [36]. Another study found that the compressive strength of 0.2% PEG-containing AAM increased to 21 MPa compared to that of reference AAM without PEG (19.5 MPa). A PEG content up to 0.6% increased the compressive strength to 22.5 MPa [37]. The combination of fly ash, eggshell powder, and rice husk ash produced high-strength geopolymer concrete. The samples were exposed to three various curing regimes: (i) AC, (ii) HC at 70°C, and (iii) SC conducted with the addition of 1% of PEG 6000. The HC exhibited the highest mechanical properties, but the results of the SC regime were close to those of HC [26].

In literature reviews, the focus was on SC regimes of AAMs, although fly ash, metakaolin, rice husk ash, and granulated blast furnace slag aluminosilicate sources are predominantly used; research on the use of natural pozzolanic aluminosilicate precursors is quite limited. On the other hand, in the previous study [38], an attempt was made to improve the material properties of natural pozzolan-based AAM by applying various curing regimes: HC, MWC, and hybrid curing (HC + MWC and MWC + HC). The strength obtained after MWC at 90 W for 15 minutes was higher than that obtained after HC at 90°C for 24 hours. Hybrid curing regimes achieved a higher reaction degree than HC or MWC alone. The highest mechanical strength was obtained by applying 24 hours of HC and 15 minutes of MWC [38]. However, these curing regimes led to poorer environmental efficiency because of higher energy consumption and CO_2 emissions. Therefore, this experimental study aimed to investigate alternative curing regimes that reduce the energy consumed during production without compromising the mechanical properties of the natural pozzolan-based AAM. The efficiency of (i) AC, (ii) WC, and (iii) SC regimes on the properties of the AAM samples was investigated. The findings were compared with the results of the HC (at 90°C for 24 hours) and MWC (at 90 W microwave power for 15 minutes) curing regimes applied in the previous study, and the effectiveness of the SC was examined compared to the other curing regimes.

2. Materials and methods

2.1. Raw materials

Low calcium-based, natural Datça Pozzolan (DP) from Türkiye was used as an aluminosilicate precursor. The largest particle size of the DP, which was ground in a ball mill to accelerate the reaction development with an alkaline solution, was 100 μm. The specific gravity determined according to ASTM D854-10 [39] was 2.52. The chemical composition of DP was determined using Philips 71 PW-2404 model X-ray fluorescence spectrometry, and is given in Table 1. More than 90 wt% of the DP composition comprised SiO_2 and Al_2O_3, the essential oxides required to develop alkaline activation reactions. Since the CaO content in its composition (1.22 wt%) is less than 10 wt% [40], DP is a low-calcium-based aluminosilicate source.

Table 1. Chemical composition of DP.

Oxide Content (wt%)	DP
SiO_2	75.29
Al_2O_3	15.99
Fe_2O_3	0.98
CaO	1.22
MgO	0.62
K_2O	3.02
SO_3	0.10
Na_2O	2.21

Table 2. Mixing ratios used in sample production.

	DP (kg)	SS (kg)	KOH (kg)	Standard sand (kg)	Total water (kg)	PEG-400 (kg)
	486.8	104.3	41.7	1460.4	131.4	4.86
Specific gravity	2.52	1.30	1.05	2.65	1.0	1.12

Alkaline activators were a mixture of commercially available potassium hydroxide (KOH) flakes with a purity of 99% and sodium silicate liquid (SS = Na_2SiO_3). KOH flakes with a specific gravity of 1.05 were dissolved in water to make a 10 molar (10 M) KOH solution. The molecular weight of KOH solid is 56.1. 10 M KOH solution consists of 10 × 56.1 = 561 g of KOH pellet per liter of the solution. The KOH solution was prepared 24 hours before being used in the AAM mixture and was cooled in a closed glass container until it reached room temperature. SS, with a specific gravity of 1.30, consisted of 7.5% Na2O, 25.5% SiO_2, and 67.0% water by mass in its chemical composition.

For the production of AAM, standard CEN sand, with specific gravity 2.65, unit weight 1.70 g/cm^3, and maximum particle size 2 mm, following TS EN 196-1 [41], was used as an aggregate.

PEG 400 is one of the most commonly used water-soluble polymers, with the formula $HO(C_2H_4O)nH$. The material, with a phase transition temperature ranging from 20°C to 35°C, is referred to as a phase change material [28]. It is a colorless, viscous liquid found in many different pharmacological compounds due to its low toxicity. PEG is a water-retention component in binders, adhesives, and ceramics [42]. PEG was obtained from a commercial company (Ataman Chemicals) and used only in SC-based samples. It has an average molecular weight of 380–420 g/mol, a specific gravity of 1.12 at 27°C, a unit weight of 1.11 g/cm^3 at 20°C, and a hydroxyl value of 300 mg KOH/g [43].

2.2. Mixing ratios for AAM

The raw material mixing ratios used in the present study were kept constant, as this formulation provided the highest mechanical properties in the previous study [38]. SS to KOH was fixed at 2.5, the total alkaline solution to DP ratio was fixed at 0.30, and the standard sand to DP ratio was kept constant at 3.0, by weight. The amount of water to produce a workable consistency without leakage from the molds was determined with a flow table test following ASTM C 1437–20 [44]. The optimum flow, where no water leakage from the edges of the mold was found, was 100% for AAM. Therefore, the total water to DP was calculated as 0.27. The mixing ratios used in the sample production are given in Table 2.

AAMs may include large amounts of water-soluble polymers. However, since a 1% addition of such polymer significantly increases the material's compressive strength (above 29%), higher concentrations are not required [45]. Therefore, in the samples exposed to the SC regime, the dosage of PEG was maintained at 1% of the weight of the aluminosilicate precursor (DP), by the recommendations obtained from the literature.

2.3. Manufacturing procedure of AAM

DP and sand were mixed for approximately five minutes. Subsequently, SS and KOH were mixed with this dry mixture within another five minutes until a homogeneous mortar was produced. PEG 400 was incorporated and mixed in samples cured with an SC regimen for three minutes. To avoid adhesion with the AAM, oil was applied on the interior surfaces of the molds before casting. Afterwards, the prismatic molds of 40×40×160 mm were filled with fresh mixtures in three layers; every layer was tightly compacted. All samples were coated with polyethylene (PE) after molding and subjected to pre-curing under AC conditions at 20 ± 2°C and 65 ± 5% RH for 24 hours. Afterwards, the samples were demolded and subjected to different curing regimes, as shown below:

- AC at 20 ± 2°C and 65 ± 5% RH for 7, 28, 90, 180, and 365 days
- WC in a water tank at 20 ± 2°C for 7, 28, 90, 180, and 365 days
- SC at 20 ± 2°C and 65 ± 5% RH for 7, 28, 90, 180, and 365 days

The production stages of natural pozzolan-based AAMs cured at various curing regimes are given in Fig. 1.

2.4. Testing procedure for AAM samples

The flow table test is one of the required tests for assessing the AAMs' workability. The test was conducted according to the guidelines given in ASTM C 1437–20 [44]. A truncated conical mold measuring 70 mm in diameter at the top, 100 mm at the bottom, and 50 mm in height was filled with fresh AAM. After that, the AAM was tampered with 20 times. The mold was lifted from the mortar, and the table was dropped

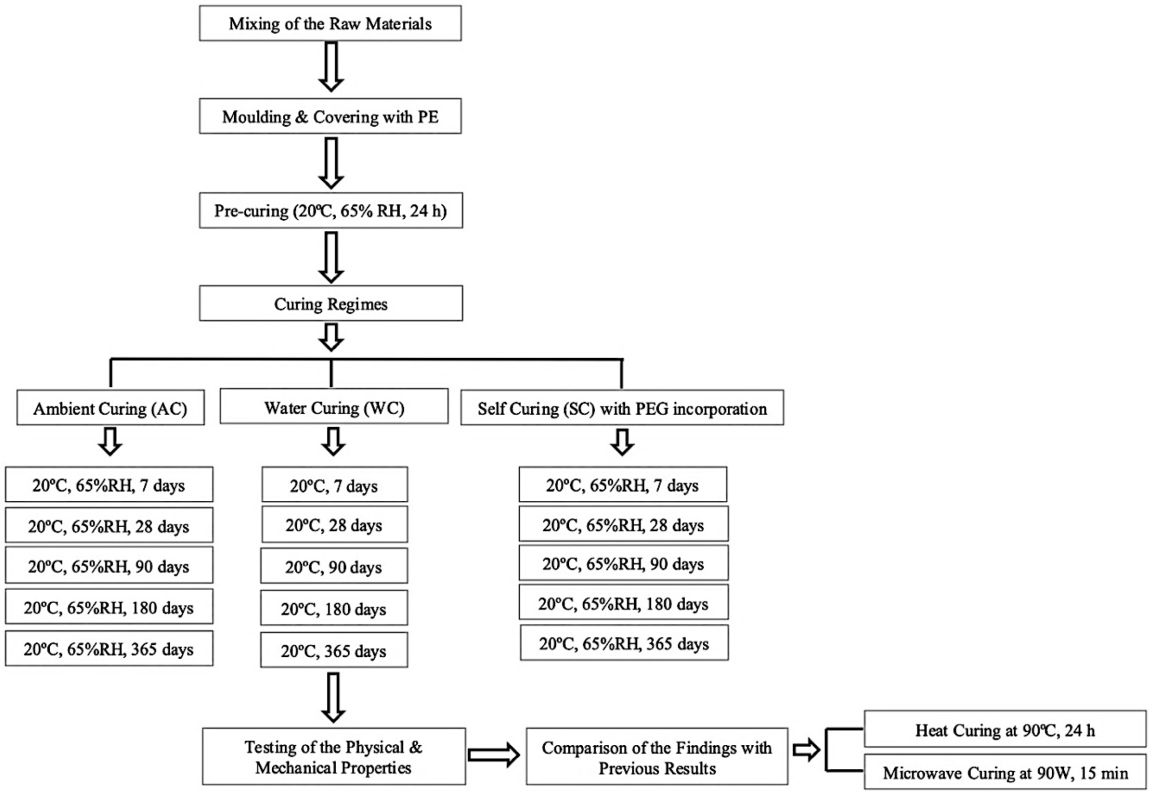


Fig. 1. Production stages of natural pozzolan-based AAMs cured using a range of regimes.

25 times in 15 s. The flow value is the resulting increase in base diameter of the material, expressed as a percentage of the original base diameter.

The samples' unit and specific weight should be measured to determine the porosity values. To calculate the unit weight, the weights of the dried samples (m_d), after drying at 100°C for 36 hours; water-saturated samples (m_s) after storing them in a water tank for 48 hours; and suspended samples (m_h) in a container filled with water were measured. The unit weight (ρ, g/cm^3) was calculated following TS EN 1015-10 [46] by using Eq. (1):

$$\rho = \left(\frac{m_d}{m_s - m_h}\right) \tag{1}$$

The specific weight (ρ_r, g/cm^3) was measured according to TS 699 [47]. Finely ground AAM was added to a glass container filled with water and allowed to settle at the bottom without air bubbles. Eq. (2) was used for the calculation:

$$\rho_r = \frac{m_{kn} - m_k}{(m_{kn} - m_k) - (m_{kns} - m_{sd})} \tag{2}$$

Where "m_k" is the weight of the empty glass container, "m_{kn}" is the weight of the container filled with the sample, "m_{sd}" is the weight of the container filled solely with water, and "m_{kns}" is the weight of the container filled with both water and the sample.

Porosity (P, %) was calculated by using Eq. (3):

$$P = \left[1 - \left(\frac{\rho}{\rho_r}\right)\right] \times 100 \tag{3}$$

Resistance to capillary suction (sorptivity test) was determined per TS EN 1925 [48]. The samples were covered with wax on the edges and placed on the supports in a water tank to absorb water only from the base. Their weights were recorded at 1, 4, 9, 25, 36, 49, 64, and 81 minutes. The water sorptivity (S, cm/$\sqrt{s}$) was calculated by using Eq. (4):

$$S = \frac{m_i - m_d}{A \times \sqrt{t_i}} \tag{4}$$

Where "m_d" is the weight of the dried sample in g, "m_i" is the successive weight of the sample at specified time intervals in g, "A" is the area of the base of the sample in m^2, and "t_i" is the time elapsed from the beginning of the test until the times at which the successive masses were measured.

A Proceq instrument automatically determined the ultrasound velocity (UV, km/s) in compliance with TS EN 14579 [49]. By placing probes at both ends of the samples, the instrument calculated it by using Eq. (5):

$$UV = \frac{L}{\mathrm{t}} \tag{5}$$

Where "L" is the sample length and "t" is the time until the sound wave is received by the receiving probe of the instrument, in μs.

Compressive and flexural strength tests were applied according to TS EN 196-1 [41] with UTEST 2000 kN (50 N/s) equipment. Compressive strength (C_s, MPa) and flexural strength (F_s, MPa) were calculated by using Eqs. (6) and (7), respectively:

$$C_s = \frac{F_c}{\mathrm{A}} \tag{6}$$

$$F_s = \frac{1.5 \times F_f \times \mathrm{I}}{b \times h^2} \tag{7}$$

Where "F_c" and "F_f" are the maximum compression and flexural loads the sample receives, in N, "A" is the area of the cross-section of the sample, in mm^2, "I" is the distance between the support cylinders, "b" is the edge length of the square cross-section of the sample, in mm, and "h" is the height of the sample, in mm.

Comprehensive methods were applied to determine the progress of alkali activation reactions. One of these methods is to dissolve the AAMs in hydrochloric acid at ambient temperature [50]. Approximately 1 gram of the ground sample was mixed with a 1:20 volume ratio of HCl to sample. Then, this mixture was filtered through paper. The resulting sediment was dried after being cleaned with water to raise the pH to 7. Eq. (8) was used to calculate the degree of reaction (DoR, %) [51]:

$$DoR = 100 - \left(\frac{m_i - m_f}{m_i}\right) \times 100 \tag{8}$$

"m_i" and "m_f" are the initial and final weights of the sample, respectively, before and after the test.

All physical and mechanical tests used prismatic samples with dimensions 40×40×160 mm. The test findings were derived from the average values of the three samples. These findings were compared with the previous research results for the same samples produced by HC at 90°C for 24 hours and with MWC at 90 W microwave power for 15 minutes.

3. Test results and discussion

3.1. The effect of curing regimes on the properties of AAM

3.1.1. Fresh-state properties

The mechanism of alkaline activation is described in the following stages: dissolution after alkaline hydrolysis (destruction), transport of cations (reorientation), and polycondensation of free silicate and aluminate components (hardening) [52]. Depending on the calcium content of the aluminosilicate precursor, two kinds of binding gels are produced in AAMs after these stages. C-A-S-H-type gels are made in Ca-rich environments using a procedure similar to that by which C-A-S-H gel forms in OPC. Polycondensation processes form sodium alumina silicate hydrate (N-A-S-H) gel in Ca-poor environments. Water is a component of C-A-S-H structures through hydration processes. In contrast, water is only needed as a dissolving medium for N-A-S-H gels and is released after the production of these gels, following polycondensation [45]. Therefore, the N-A-S-H gels are not chemically bonded to water in low Ca-based AAMs. It is essential for the dissolution stage of the alkaline activation reactions to use alkaline solutions as the reaction medium and to provide the "workability" to be easily produced, transported, placed, and compacted without any segregation. Thus, workability is an essential physical property of AAMs. The comparison of flow table test results of AAM subjected to AC and WC (without PEG) and AAM subjected to SC (with PEG) is shown in Fig. 2 as an indication of the workability. The test results found that PEG incorporation increased the flow value from 100% to 115%, by 15%. Thus, adding PEG improved the workability of the natural pozzolan-based AAMs by maintaining the moisture content of the matrix, which facilitates the ideal curing conditions, especially in hot and dry climatic regions.

3.1.2. Hardened-state properties

Figs. 3 and 4 depict the evolution of the physical and mechanical properties of natural pozzolan-based AAMs cured using various regimes.

In all curing periods, the samples subjected to WC exhibited the highest porosity and the lowest unit weight, followed by AC and SC, respectively. The porosity and unit weight of the samples subjected to WC for seven days were 22.17% and 1.73 g/cm^3, respectively. The porosity decreased by 6.1% to 20.81%, and the unit weight increased by 3.4% to 1.79 g/cm^3 when the samples were subjected to AC for the same curing period. After subjecting the samples to SC for seven days, the porosity decreased by 18.4%, and unit weight increased by 4.0%

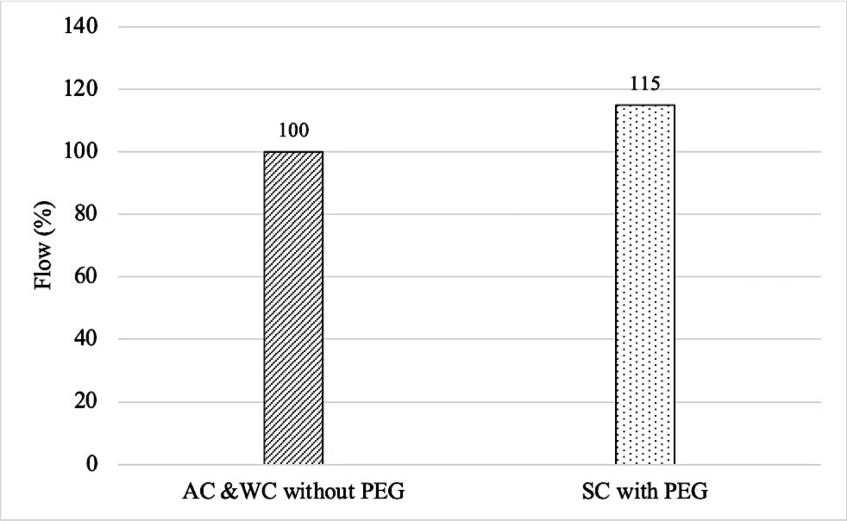


Fig. 2. The flow values of the natural pozzolan-based AAMs.

compared to WC. These findings identified in the physical properties were also reflected in the improvement in the mechanical properties (Fig. 4). The lowest compressive strength (2.31 MPa), flexural strength (0.89 MPa), and ultrasound velocity (0.63 km/s) were observed in the samples subjected to WC for seven days. By subjecting the samples to AC and SC during the same curing period, the compressive strength increased by 26.8% and 40.7%, the flexural strength increased by 41.5% and 116.8%, and the ultrasound velocity increased by 30.1% and 44.4%, respectively, compared to those of the WC. These improvements found in the properties suggest that AC and SC provide more favorable curing conditions for producing AAM with a more compact internal structure. These character enhancements imply alkaline activation processes are more complete after AC and SC. The effectiveness of the increased curing period on the development of properties is discussed in the next section.

Determination of the lowest properties in water showed that WC may hinder the development or process of the reactions. A potential cause of this was that the leaching of alkaline activators into the water made it unavailable to activate the AAM [22]. Unlike with OPC, curing AAM with water reduces the alkaline concentration in the matrix. The alkaline solutions required for the reactions (KOH and SS) leached out of the pores due to the water immersion. With increases in the curing period, a higher quantity of KOH solution was reported to be expelled [53], and the alkaline activation reactions were partially inhibited. Thus, lower amounts of binding gels were created, leading to higher porosity and lower mechanical strength. The previous studies agreed on these findings [22, 53, 54].

The samples subjected to SC found the lowest porosity and the highest unit weight values. The porosity of the SC-cured samples for seven days was 18.08%, which was 13.1% lower than the porosity of the AC-cured samples. Similarly, the compressive strength (3.25 MPa), flexural strength (1.93 MPa), and ultrasound velocity (0.91 km/s) of the same samples were 10.9%, 53.1%, and 10.9% higher, respectively, compared to those cured with AC. This enhancement, brought about by the inclusion of PEG, was notable and was consistent with other published findings that reported on the combination of metakaolin and PEG [55]. This property's enhancement might result from forming H-bonds between -OH groups of the inorganic AAM matrix and the ethereal oxygen atoms and/or terminal alcoholic groups in the PEG chain. In addition, the inorganic matrix underwent reorganization, which increased Al-O-Si bonds over time, as the alkaline activation reactions proceeded. Thus, PEG's presence affected the reactions' evolution and resulted in the development of an aluminosilicate network, rich in Si-O-Al bonds [55]. The increase in properties might also be due to the PEG retaining more moisture in the matrix. This retention was necessary for the appropriate dissolution stage of the alkaline activation reactions and contributed to higher strength. Such a change in the microstructure was also compatible with the development of the physical properties. A similar trend in water sorptivity was also observed in porosity, as shown in Fig. 5. The 7-day SC decreased water sorptivity by 13.3% and 7.4%, compared to WC and

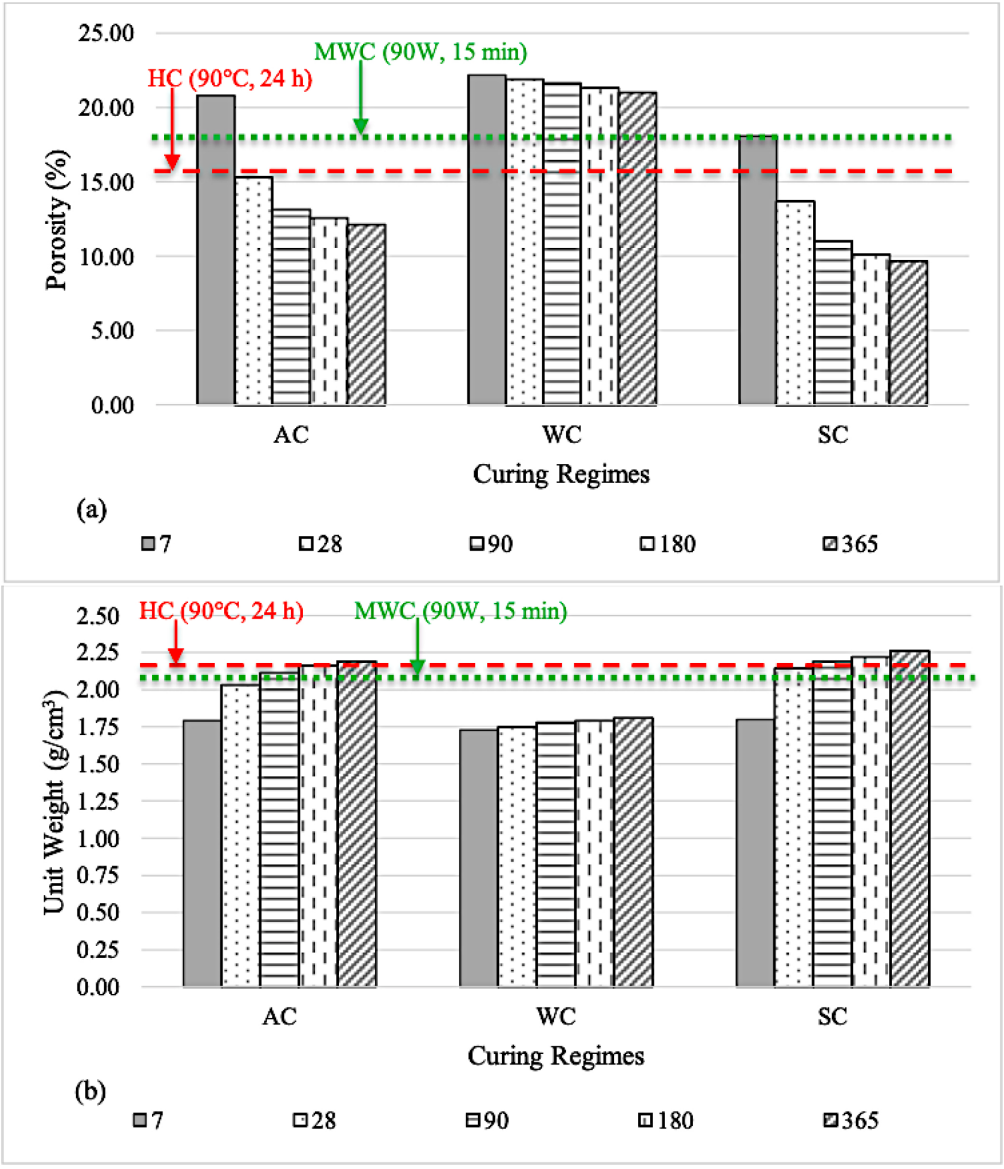


Fig. 3. The physical properties of natural pozzolan-based AAMs cured with various curing regimes: (a) Porosity; (b) Unit weight.

AC, respectively. This means that SC-cured samples exhibited better performance in terms of resistance to water penetration (by capillary suction) due to their better microstructure modification.

The test results of this study were compared with the previous findings on the samples with the same mixing ratio but cured by HC and MWC regimes (Figs. 3 and 4). The porosity of samples cured with WC in the present study was higher than that of samples subjected to HC (90°C, 24 hours) or MWC curing (90 W, 15 minutes), while the unit weight was lower. Similarly, the compressive and flexural strengths and ultrasound velocity of the WC-cured samples did not meet the values achieved by HC or MWC. Thus, the WC is the least suitable curing regime for producing natural pozzolan-based AAM. Furthermore, the results obtained with seven days of AC failed to meet previously obtained values with HC or MWC. However, by increasing the AC curing period from seven days to 28 days, the porosity decreased to that of the samples cured with HC and MWC, and the unit weight increased to the value obtained with HC and MWC. Similarly, the compressive strength obtained with 28 days of AC was essential for providing results of the samples cured in both HC and MWC regimes. The flexural strength and ultrasound velocity after 28 days of AC could meet the values obtained with MWC. In other words, the material properties obtained with HC for 24 hours or MWC for 15 minutes are achievable with AC in 28 days

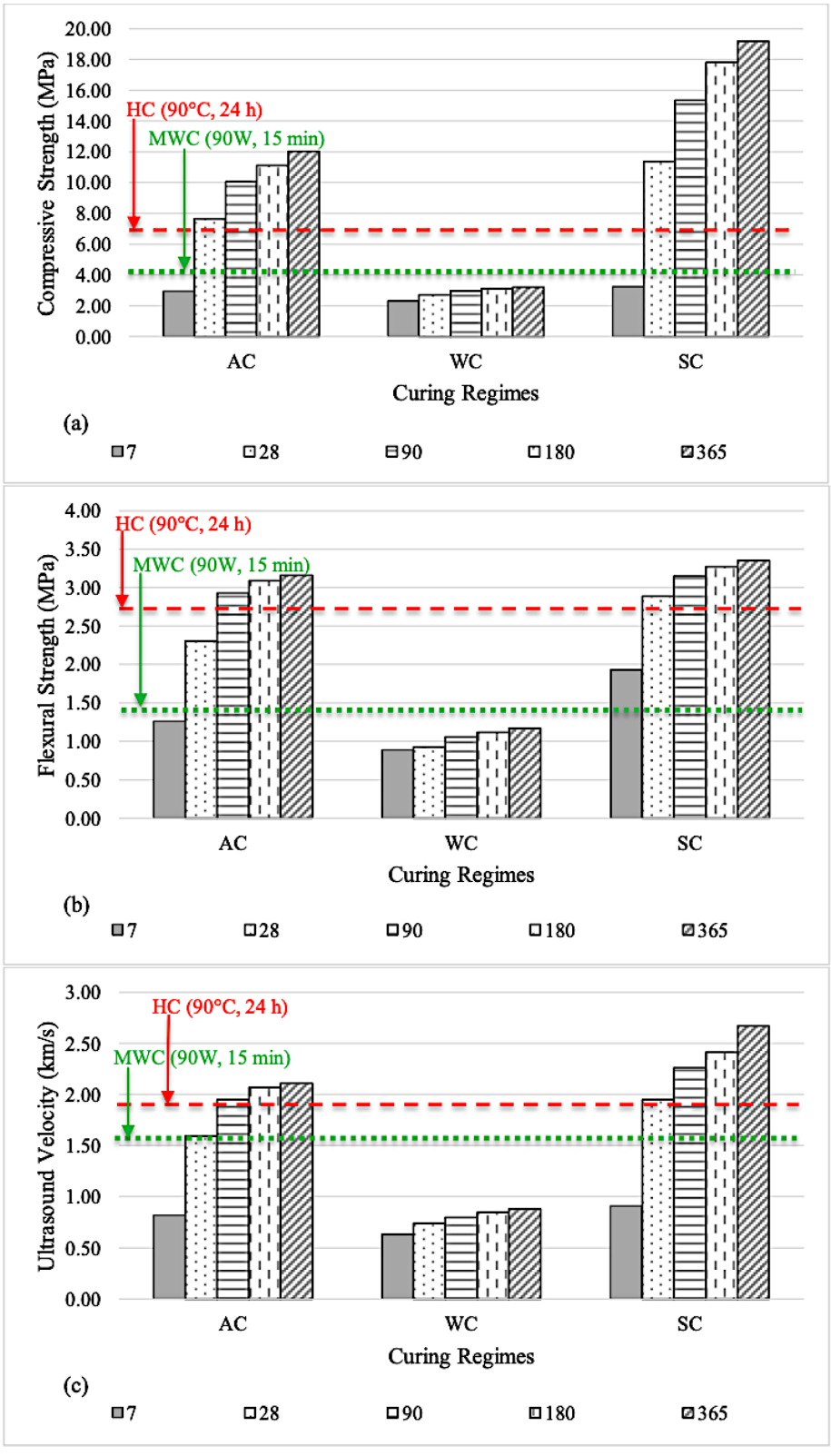


Fig. 4. The mechanical properties of natural pozzolan-based AAMs cured with various curing regimes: (a) Compressive strength; (b) Flexural strength; (c) Ultrasound velocity.

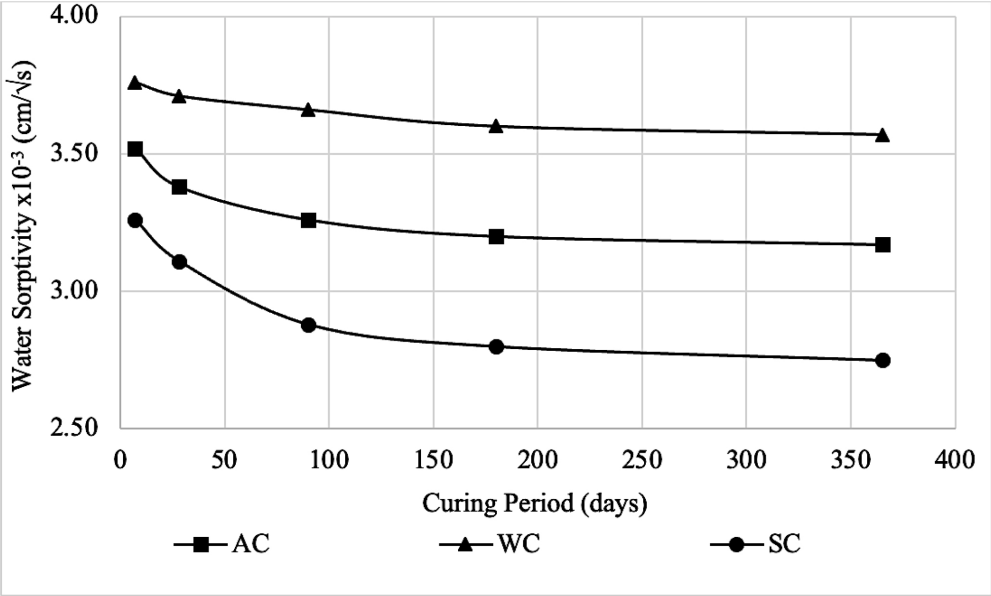


Fig. 5. Graph of water sorptivity values as a function of curing period.

without additional energy expenditure. The higher mechanical properties were achieved by gradually increasing the AC curing period from 28 days to 90, 180, and 365 days, surpassing the values obtained with HC and MWC.

When comparing the effectiveness of SC with HC and MWC, the seven days of SC matched the porosity value of samples produced with both HC and MWC in the earlier study. The further decrease in porosity with the extension of the SC curing period beyond 28 days demonstrated the positive effect of an SC regime on the internal structural development of AAM. The higher values of the mechanical properties observed in SC-cured samples for 28 days, compared to HC and MWC, revealed superior SC performance in producing natural pozzolan-based AAM. The highest properties were observed in samples cured with SC for 365 days. The values obtained for this specific regime were: 9.69% of porosity, 2.26 g/cm^3 of unit weight, 2.75×10^{-3} cm/$\sqrt{s}$ of water sorptivity, 19.20 MPa of compressive strength, 3.35 MPa of flexural strength, and 2.67 km/s of ultrasound velocity. Since these values were much higher than those of HC- or MWC-curing, AAM might be optimally produced by adding PEG but without using energy-consuming curing techniques.

3.2. The effect of curing period on the properties of AAM

"Relative physical and mechanical properties" refers to characteristics expressed compared to a reference value. In the current study, each relative material property was calculated by dividing the values obtained on the 28th, 90th, 180th, and 365th days by the values obtained on the 7th day. These properties of AAMs produced with various curing regimes as a function of curing period are shown in Fig. 6.

As the curing period progressed, the properties of the AAM improved. This increasing trend was highest in SC-cured samples, followed by AC and WC. As the curing period increased from seven days to 28 and 90 days, the porosity of SC-cured samples decreased by 0.76 times and 0.61 times, respectively, while the unit weight (1.19 and 1.22 times), the compressive strength (3.50 and 4.72 times), the flexural strength (1.59 and 1.78 times), and the ultrasound velocity (2.21 and 2.71 times) increased. The 0.95-fold and 0.88-fold reduction in water sorptivity values was another indication that the AAM structure became more resistant to water over time (Fig. 5). Similarly, as a result of 28 and 90 days of AC, the porosity of the samples decreased by 0.79 and 0.63 times, respectively. The water sorptivity decreased by 0.96 and 0.93 times, while the unit weight increased by 1.13 and 1.18. Concurrently, the compressive strength increased by 3.16 and 4.14 times, the flexural strength increased by 1.50 and 1.63 times, and the ultrasound velocity increased by 2.14 and 2.48 times, respectively, compared to the results after seven days of curing. The higher strength of an AAM may be closely related to its better-developed microstructure and lower porosity. In contrast, increasing the WC curing period beyond the seventh day did not cause any significant changes in the properties. This was probably due to the greater leaching of KOH solution

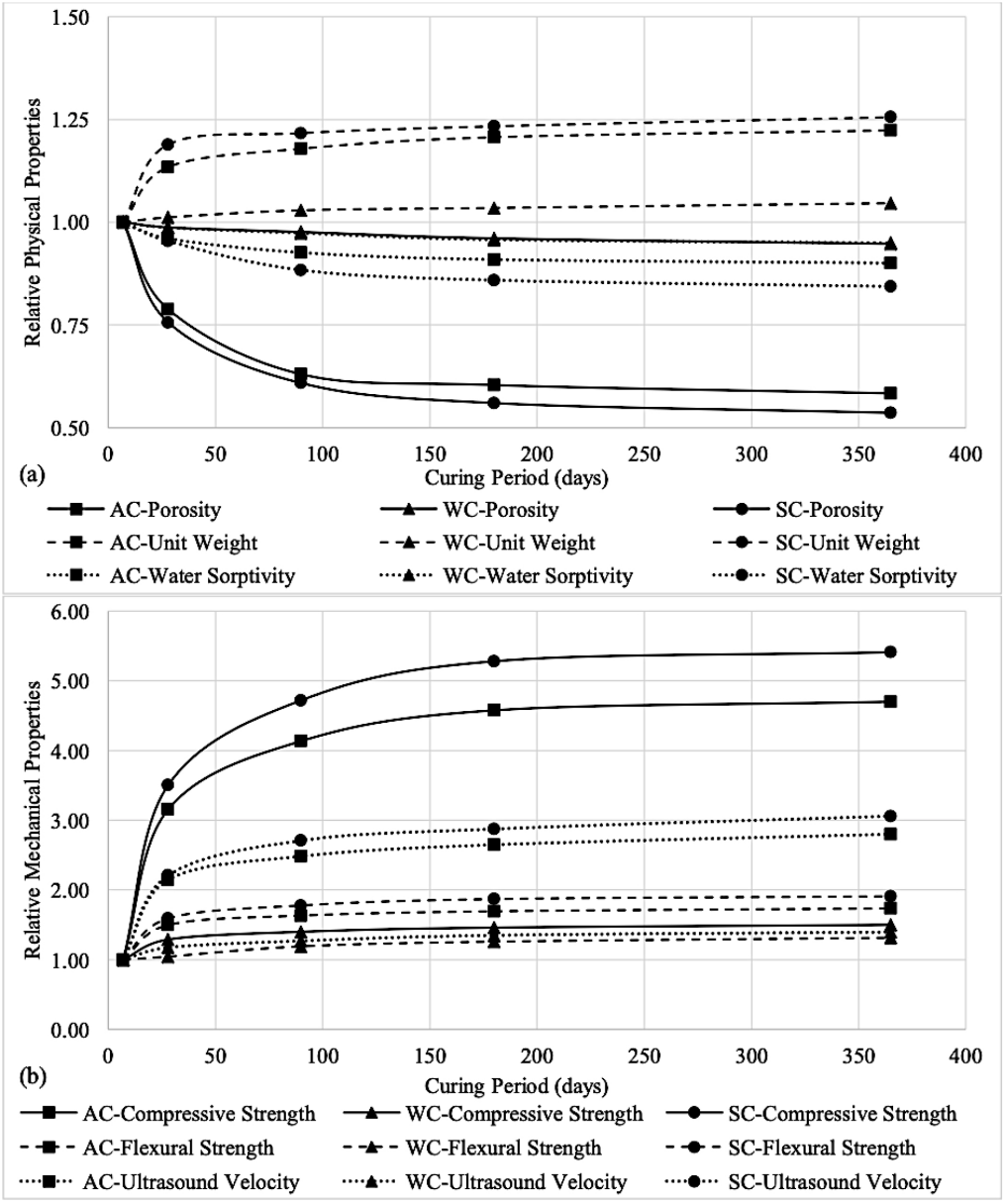


Fig. 6. Relative properties of the AAMs as a function of curing period: (a) Physical properties; (b) Mechanical properties.

from the pores of the samples over a more extended period, as discussed above, and the consequent inhibition of alkaline activation reactions [53]. Since the optimal amounts of alkaline solution required to develop the reactions were not present within the matrix, a lower amount of binding gel was formed. Thus, the increased WC curing period did not enhance the properties of AAM.

The positive changes detected in the properties of the AAMs, especially under the AC and SC curing regimes, revealed that the material developed a more compact microstructure over time. As shown in Fig. 6, the slope of the curing period curve for relative physical and mechanical properties was steep between 7 and 28 days, indicating that the reaction development of AAM and the formation of internal structure were rapid during this period. The slope of the curve between 28 and 90 days was shallower than the slope between 7 and 28 days. Especially in the curing period after 90 days, the curve had plateaued, indicating that the first 90 days were more effective in the development of the internal structure of the AAM, and more meaningful development was not evident between 90 and 365 days. The significantly higher rate of increase in the relative properties of SC-cured samples demonstrated the effectiveness of PEG

Table 3. Comparison of the 28-day compressive and flexural strengths of AAMs produced with PEG or without PEG incorporation.

			Compressive Strength (MPa)			Flexural Strength (MPa)		
Ref	Precursor Type	PEG Content(%)	Ref. (without PEG)	With PEG	Increasing ratio (%)	Ref. (without PEG	With PEG	Increasing ratio (%)
[28]	Metakaolin	1, 2, 3% PEG 400	28^{th} days = 20.1	1%PEG =∼ 32.5 2%PEG =∼ 37.1 3%PEG =∼ 35	61.7 84.5 74.1	28^{th} days = 3.7	1%PEG =∼ 6.5 2%PEG =∼ 7.2 3%PEG =∼ 7.0	75.6 94.5 89.1
[36]	Metakaolin	0.5, 1, 2, 5, 7, 10% PEG 400	28^{th} days = ∼ 16.1	1%PEG =∼ 13.5 2%PEG =∼ 14.6 5%PEG =∼ 20.5 7%PEG =∼ 20 10%PEG =∼ 23.9	–16.1 –9.3 27.3 24.2 49.3	28^{th} days =∼2	1%PEG = 1.8 2%PEG =∼ 1.9 5%PEG =∼ 2.3 7%PEG =∼ 2.25 10%PEG =∼ 2.9	–10 –5 15 12.5 45
[37]	Kaolin	0.2, 0.6 %PEG400	28^{th} days = ∼19.5	0.2%PEG =∼ 21 0.6%PEG =∼ 22.5	7.7 15.3	– –	– –	– –
[26]	Fly ash + eggshell powder, rice husk ash	%1PEG 600	28^{th} days =∼ 80	1%PEG =∼ 85	6.2	28^{th} days =∼ 11	1%PEG =∼ 13	18.1
This study	Natural pozzolan	%1PEG400	28^{th} days = 7.67	1%PEG = 11.39	48.5	28^{th} days = 2.30	1%PEG = 2.89	25.6

addition in improving the internal structure development of AAM, both in the early and later stages. In the 90, 180, and 365-day curing periods, the highest mechanical properties were observed in the SC-curing, followed by the AC- and WC-curing.

Table 3 compares the 28-day compressive and flexural strengths of AAMs produced with or without PEG incorporation. In the present study, adding 1% PEG (SC) increased the compressive strength by 48.5% and the flexural strength by 25.6% compared to the samples produced with AC for 28 days. This rate of increase in compressive strength was higher than the rates of growth of kaolin-based AAMs containing 0.2% and 0.6% PEG [37], fly ash + eggshell powder + rice husk ash-based AAMs containing 1% PEG [26], and metakaolin-based AAMs containing 1%, 2%, 5%, and 7% PEG [36]. Still, it was in a similar range to metakaolin-based AAMs containing 10% PEG [36]. The increase in flexural strength rate was lower than that of metakaolin-based AAMs containing 1%, 2%, or 3% PEG [28] and 10% PEG [36]. It was higher than those reported for metakaolin-based AAMs containing 1%, 2%, 5%, or 7% PEG [36] and fly ash + eggshell powder + rice husk ash-based AAMs containing 1% PEG [26]. The findings obtained in this study are consistent with the results of other published studies and demonstrate that SC may best produce natural pozzolan-based AAM with PEG incorporation. However, the effects of various PEG contents on the properties of these AAMs should be determined in future research.

3.3. The effect of curing regimes and curing period on the degree of reaction

The degree of reaction of AAMs cured at various curing regimes is given in Fig. 7a. In all curing periods, the highest degree of reaction was detected in the samples subjected to SC, followed by AC and WC. The degree of reaction of the samples cured with WC for 7 days was 2.21%. The degree of reaction increased by 80.9% (4.00%) and 152.9% (5.59%) when the samples were subjected to AC and SC, respectively, for the same curing period. From these improvements, it can be implied that AC and SC were more favorable regimes for producing AAM. The highest degree of reactions (5.59%, 13.25%, 14.60%, 15.21%, and 15.42% after 7, 28, 90, 180, and 365 days, respectively) was found in the SC-cured samples. The degree of reaction results of the present study was compared with the previous research results on the samples cured by the HC and MWC regimes. The degree of reaction of the samples cured with WC did not meet the values provided by HC or MWC for any curing period. The degree of reaction of the samples cured with seven days of AC and SC failed to achieve the values obtained with either HC or MWC. However, by increasing the AC curing period from seven to 28 days, the degree of reaction value (11.16%) was significant compared to the results of both HC and MWC. This means that the evolution of the reactions obtained in 24 hours with HC, or in 15 minutes with MWC, could again be achieved in 28

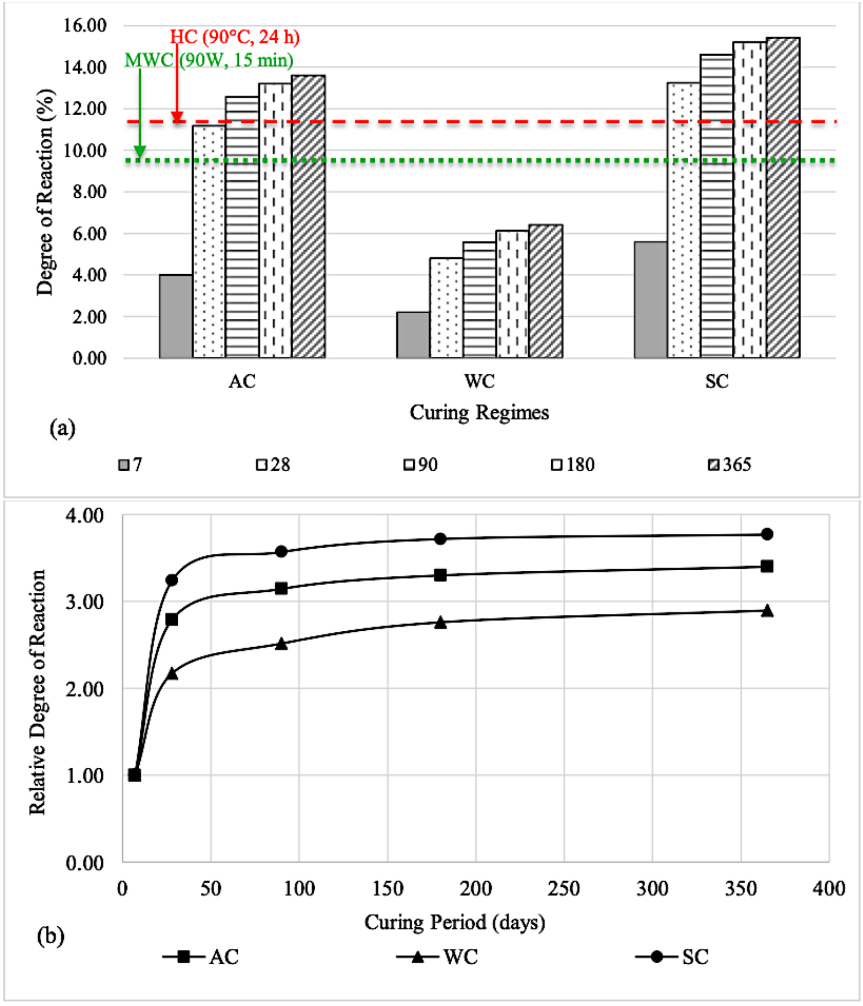


Fig. 7. (a) The degree of reaction of natural pozzolan-based AAMs cured using various curing regimes; (b) Graph of relative degree of reaction as a function of curing period.

days with AC. The degree of reaction after 28-day SC was higher than that of HC or MWC, indicating that PEG incorporation may accelerate alkaline activation reactions and could also cause an increase in the extent of reaction. Indeed, these findings were significant because they are consistent with the mechanical properties mentioned in the previous section.

As shown in Fig. 7b, the degree of reaction also changed during the study period (7–365 days). The degree of reaction of all samples was exceptionally high between seven and 28 days, indicating the reaction development of AAM and the rapid formation of internal structure. This increasing trend meant that until the activating solution consumed all of the readily available substrate, the degree of reaction continued to increase. However, the growing ratio of the degree of reaction decreased between 28 and 90 days in all samples. Especially after 90 days, the curve again tended to plateau, showing that the first 90 days were more effective in developing alkaline activation reactions, as suggested in the previous section.

The compressive strength of the AAMs as a function of the degree of reaction is given in Fig. 8. The compressive strength increased with the degree of reaction in all samples. The AAM cured with SC exhibited the most significant effect, followed by the AC and WC samples. The slopes of the regression lines decreased slowly in the order of SC (0.80), AC (0.74), and WC (0.15). The greater slopes of SC and AC indicated a higher rate of strength development as a function of the degree of reaction. In addition, the magnitude of the correlation coefficients was relatively high (R^2: 0.99) in all curing regimes. From these findings, the compressive strength of natural pozzolan-based AAMs may be estimated through their degree of reaction. The linear correlation between the compressive strength and degree of reaction can be expressed by the following

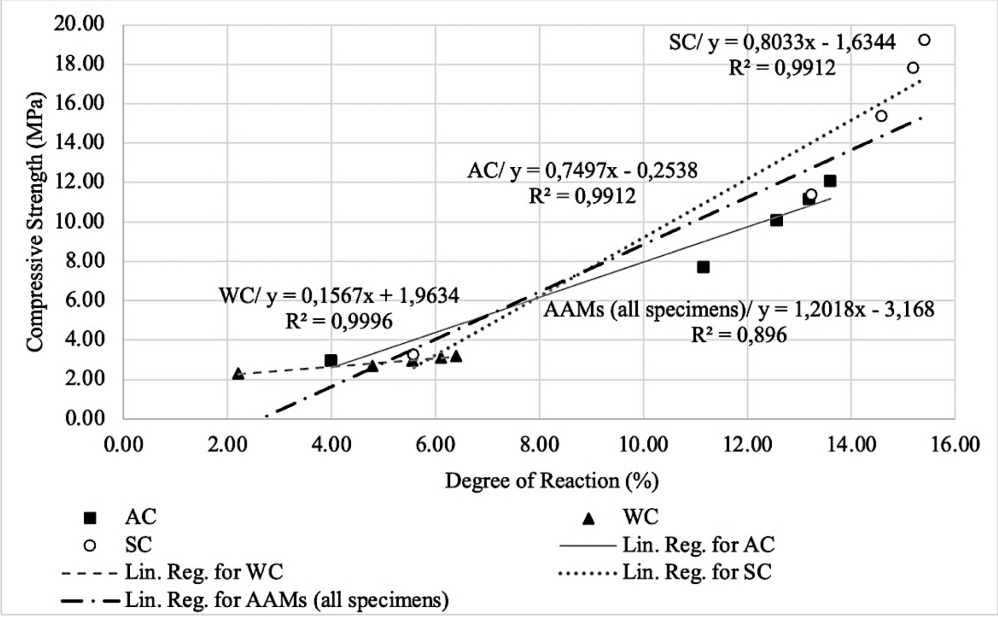


Fig. 8. The compressive strength of the AAMs as a function of the degree of reaction.

Eq. (9):

$$C_s = (a \times DoR) + b \quad (9)$$

"a" gives the slope of the regression lines, which are 0.80 (for SC), 0.74 (for AC), 0.15 (for WC), and 1.20 for all AAM samples. "b" is –1.63, –0.25, 1.96 for SC, AC, and WC, and –3.1 for all samples, as expressed by the following Eqs. (10) to (13):

$$(WC)\ C_s = (0.1567 \times DoR) + 1.9634 \quad (10)$$

$$(AC)\ C_s = (0.7497 \times DoR) - 0.2538 \quad (11)$$

$$(SC)\ C_s = (0.8033 \times DoR) - 1.6344 \quad (12)$$

$$(All)\ C_s = (1.2018 \times DoR) - 3.168 \quad (13)$$

4. Conclusion

Some specific conclusions are summarized as follows:

- Although AC and SC are alternative curing regimes that can be applied in producing natural pozzolan-based AAMs, WC is unsuitable because it does not positively affect the material properties at early or later periods.
- PEG 400 appears to be highly effective and can produce natural pozzolan-based AAMs.
- PEG incorporation increased the AAM's workability, making SC a favorable curing regime, especially in hot and dry climatic regions. The highest degree of reaction, physical and mechanical properties, was observed in SC-cured samples in the early period and up to 365 days.
- Applying 28-day AC or SC instead of energy-intensive HC (90°C for 24 hours) and MWC (90 W for 15 minutes) is an alternative method in producing natural pozzolan-based AAM. Future studies should investigate using various mixing ratios to shorten the 28-day curing period without compromising the material's mechanical properties.
- Applying SC without any additional curing energy consumption and higher CO_2 emissions compared to other energy-intensive regimes may provide *in-situ* practical advantages that enable the large-scale application of AAMs.
- Increasing the curing period from seven days to 28 and 90 days significantly improved the physical and mechanical properties. However, from 90 days to 365 days, the rate of increase in the properties was lower than in the early period.
- A high linear correlation between compressive strength and degree of reaction of the AAMs indicates that the compressive strength can be estimated through the degree of reaction.
- To enable the use of natural pozzolan-based AAMs in the construction sector, the effectiveness of various weathering agents, such as wetting-drying, freeze-thaw, and fire impact, should be experimentally investigated, and the material durability should be further determined in future studies.

Conflict of interest

The author declared no potential conflicts of interest concerning the research, authorship, and/or publication of this article.

Data availability statement

All graphs and data obtained or generated during the investigation appear in the published article.

Author's contributions

Author #1 Kübra & Ekiz Barış: Supervised the experiment's progress, performed the experiment, result analysis, and wrote the manuscript.

Ethics

There are no ethical issues with the publication of this manuscript.

References

1. Nodehi M, Ozbakkaloglu T, Gholampour A, Mohammed T, Shi X. The effect of curing regimes on physico-mechanical, microstructural and durability properties of alkali-activated materials: A review. *Construction and Building Materials*. 2022;321:126335. https://doi.org/10.1016/j.conbuildmat.2022.126335.
2. Wang W, Noguchi T. Alkali-silica reaction (ASR) in the alkali-activated cement (AAC) system: A state-of-the-art review. *Construction and Building Materials*. 2020;252:119105. https://doi.org/10.1016/j.conbuildmat.2020.119105.
3. Wang A, Zheng Y, Zhang Z, Liu K, Li Y, Shi L, Sun D. The durability of alkali-activated materials in comparison with ordinary Portland cements and concretes: A review. *Engineering*. 2020;6(6):695–706. https://doi.org/10.1016/j.eng.2019.08.019.
4. Oey T, La Plante EC, Falzone G, Hsiao YH, Wada A, Monfardini L, Bauchy M, Bullard JW, Sant G. Calcium nitrate: A chemical admixture to inhibit aggregate dissolution and mitigate expansion caused by alkali-silica reaction. *Cement and Concrete Composites*. 2020;110:103592. https://doi.org/10.1016/j.cemconcomp.2020.103592.
5. Khater HM. Effect of calcium on geopolymerization of aluminosilicate wastes. *Journal of Materials in Civil Engineering*. 2012;24(1):92–101. https://doi.org/10.1061/(ASCE)MT.1943-5533.0000352.
6. Suwan T, Fan M. Influence of OPC replacement and manufacturing procedures on the properties of self-cured geopolymer. *Construction and Building Materials*. 2014;73:551–61. https://doi.org/10.1016/j.conbuildmat.2014.09.065.
7. Rekha MS, Sumathy SR. Engineering properties of Self-cured Geopolymer concrete binded with supplementary cementitious materials. *Materials Today: Proceedings*. 2022;69(3):879–87. https://doi.org/10.1016/j.matpr.2022.07.357.
8. Provis JL, Bernal SA. Binder chemistry – Blended systems and intermediate Ca content. Provis, J., van Deventer, J. (eds). Alkali Activated Materials. RILEM State-of-the-Art Reports, 2014. 13, Springer, Dordrecht. https://doi.org/10.1007/978-94-007-7672-2_5.
9. Ruan S, Al-Mansour A, Zeng Q, Zhou X. Alkali-activated concrete via oven and microwave radiation curing. Fernando Pacheco-Torgal, Prinya Chindaprasirt, Togay Ozbakkaloglu (eds). Handbook of Advances in Alkali-Activated Concrete, Woodhead Publishing, 2022. p. 125–155. https://doi.org/10.1016/B978-0-323-85469-6.00015-5.
10. Palomo A, Grutzeck MW, Blanco-Varela M. Alkali-activated fly ashes - a cement for the future. *Cement and Concrete Research*. 1999;29(8):1323–9. https://doi.org/10.1016/S0008-8846(98)00243-9.
11. Narayanan A, Shanmugasundaram P. An experimental investigation on fly ash-based geopolymer mortar under different curing regime for thermal analysis. *Energy and Buildings*. 2017;138:539–45. https://doi.org/10.1016/j.enbuild.2016.12.079.
12. El-Hassan H, Shehab E, Al-Sallamin A. Influence of different curing regimes on the performance and microstructure of alkali-activated slag concrete. *Journal of Materials in Civil Engineering*. 2018;30(9):04018230. https://doi.org/10.1061/(ASCE)MT.1943-5533.0002436.
13. Nasir M, Johari MAM, Maslehuddin M, Yusuf MO, Al-Harthi MA. Influence of heat curing period and temperature on the strength of silico-manganese fume-blast furnace slag-based alkali-activated mortar. *Construction and Building Materials*. 2020;251:118961. https://doi.org/10.1016/j.conbuildmat.2020.118961.
14. Rostami M, Behfarnia K. The effect of silica fume on durability of alkali activated slag concrete. *Construction and Building Materials*. 2017;134:262–8. https://doi.org/10.1016/j.conbuildmat.2016.12.072.
15. Gebregziabiher BS, Thomas R, Peethamparan S. Very early-age reaction kinetics and microstructural development in alkali-activated slag. *Cement and Concrete Composites*. 2015;55:91–102. https://doi.org/10.1016/j.cemconcomp.2014.09.001.
16. Shah SFA, Chen B, Oderji SY, Haque MA, Ahmad MR. Improvement of early strength of fly ash-slag based one-part alkali activated mortar. *Construction and Building Materials*. 2020;246:118533. https://doi.org/10.1016/j.conbuildmat.2020.118533.
17. Huang G, Ji Y, Zhang L, Li J, Hou Z. The influence of curing methods on the strength of MSWI bottom ash-based alkaliactivated mortars: The role of leaching of OH and free alkali. *Construction and Building Materials*. 2018;186:978–85. https://doi.org/10.1016/j.conbuildmat.2018.07.224.
18. Mgbemena CO, Li D, Lin M-F, Liddel PD, Katnam KB, Thakur VK, Nezhad HY. Accelerated microwave curing of fibre-reinforced thermoset polymer composites for structural applications: A review of scientific challenges. *Composites Part A: Applied Science and Manufacturing*. 2018;115:88–103. https://doi.org/10.1016/j.compositesa.2018.09.012.
19. Yılmazer Polat B. The influence of microwave curing on the strength of silica fume-added fly ash-based geopolymer mortars. *Journal of Sustainable Construction Materials and Technologies*. 2023;8(3):207–15. https://doi.org/10.47481/jscmt.1315096.
20. Tan J, Cai J, Huang L, Yang Q, Mao M, Li J. Feasibility of using microwave curing to enhance the compressive strength of mixed recycled aggregate powder based geopolymer. *Construction and Building Materials*. 2020;262:120897. https://doi.org/10.1016/j.conbuildmat.2020.120897.

21. Somaratna J, Ravikumar D, Neithalath N. Response of alkali activated fly ash mortars to microwave curing. *Cement and Concrete Research*. 2010;40(12):1688–96. https://doi.org/10.1016/j.cemconres.2010.08.010.
22. Graytee A, Sanjayan JG, Nazari A. Development of a high strength fly ash-based geopolymer in short time by using microwave curing. *Ceramics International*. 2018;44(7):8216–22. https://doi.org/10.1016/j.ceramint.2018.02.001.
23. Kastiukas G, Ruan S, Liang S, Zhou X. Development of precast geopolymer concrete via oven and microwave radiation curing with an environmental assessment. *Journal of Cleaner Production*. 2020;255:120290. https://doi.org/10.1016/j.jclepro.2020.120290.
24. Chindaprasirt P, Rattanasak U, Taebuanhuad S. Role of microwave radiation in curing the fly ash geopolymer. *Advanced Powder Technology*. 2013;24(3):703–7. https://doi.org/10.1016/j.apt.2012.12.005.
25. Shi H, Ma H, Tian L, Yang J, Yuan J. Effect of microwave curing on metakaolin-quartz-based geopolymer bricks. *Construction and Building Materials*. 2020;258:120354. https://doi.org/10.1016/j.conbuildmat.2020.120354.
26. Yuan X, Xu W, AlAteah AH, Mostafa SA. Evaluation of the performance of high-strength geopolymer concrete prepared with recycled coarse aggregate containing eggshell powder and rice husk ash cured at different curing regimes. *Construction and Building Materials*. 2024;434:136722. https://doi.org/10.1016/j.conbuildmat.2024.136722.
27. Venkatesh C, Rao MVS, Kumar MP, Sonali Sri Durga C. Effect of mineral admixtures and curing regimes on properties of self-compacting concrete. *Journal of Sustainable Construction Materials and Technologies*. 2024;9(1):25–35. https://doi.org/10.47481/jscmt.1383493.
28. Vanitha N, Jeyalakshmi R. The role of polyethylene glycol, a water entrainer on characteristics of silico alumino phosphate geopolymer to harvest enhanced gel phase and stability. *Journal of Inorganic and Organometallic Polymers and Materials*. 2023;33:2835–47. https://doi.org/10.1007/s10904-023-02715-8.
29. Lokeshwari M, Pavan Bandakli BR, Tarun SR, Sachin P, Kumar V. A review on self-curing concrete. *Materials Today: Proceedings*. 2021;43(2):2259–64. https://doi.org/10.1016/j.matpr.2020.12.859.
30. Singh K. Mechanical properties of self curing concrete studied using polyethylene glycol-400: A-review. *Materials Today: Proceedings*. 2021;37(Part 2):2864–71. https://doi.org/10.1016/j.matpr.2020.08.662.
31. Pacheco-Torgal F, Moura D, Ding Y, Jalali S. Composition, strength and workability of alkali-activated metakaolin based mortars. *Construction and Building Materials*. 2011;25(9):3732–45. https://doi.org/10.1016/j.conbuildmat.2011.04.017.
32. Rattanasak U, Pankhet K, Chindaprasirt P. Effect of chemical admixtures on properties of high-calcium fly ash geopolymer. *International Journal of Minerals, Metallurgy and Materials*. 2011;18(3):364–9. https://doi.org/10.1007/s12613-011-0448-3.
33. Phoo-ngernkham T, Chindaprasirt P, Sata V, Hanjitsuwan S, Hatanaka S. The effect of adding nano-SiO_2 and nano-Al_2O_3 on properties of high calcium fly ash geopolymer cured at ambient temperature. *Materials & Design*. 2014;55:58–65. https://doi.org/10.1016/j.matdes.2013.09.049.
34. Nath P, Sarker PK. Use of OPC to improve setting and early strength properties of low calcium fly ash geopolymer concrete cured at room temperature. *Cement and Concrete Composites*. 2015;55:205–14. https://doi.org/10.1016/j.cemconcomp.2014.08.008.
35. Zhang YJ, Wang YC, Xu DL, Li S. Mechanical performance and hydration mechanism of geopolymer composite reinforced by resin. *Materials Science and Engineering: A*. 2010;527(24–25):6574–80. https://doi.org/10.1016/j.msea.2010.06.069.
36. Mikhailova O, Rovnaník P. Effect of polyethylene glycol addition on metakaolin-based geopolymer. *Procedia Engineering*. 2016;151:222–8. https://doi.org/10.1016/j.proeng.2016.07.379.
37. Zhang S, Gong K, Lu J. Novel modification method for inorganic geopolymer by using water soluble organic polymers. *Materials Letters*. 2004;58(7–8):1292–6. https://doi.org/10.1016/j.matlet.2003.07.051.
38. Barış KE. The role of microwave curing in the production of natural pozzolan-based geopolymer. *Journal of the Faculty of Engineering and Architecture of Gazi University*. 2024;39(4):2239–51. https://doi.org/10.17341/gazimmfd.1267017.
39. ASTM Standards. Standard Test Method for Gravity of Soils by Water Pycnometer, West Conshohocken, United States. ASTM D, 2010. p. 854–10.
40. Martín-Rodríguez P, García-Lodeiro I, Fernández-Carrasco L, Blanco-Varela MT, Palomo A, Fernández-Jiménez A. Artificial precursor for alkaline cements. *Composites Part B: Engineering*. 2025;296:112216. https://doi.org/10.1016/j.compositesb.2025.112216.
41. Turkish Standard Institution. Methods of Testing Cement - Part 1: Determination of Strength. Ankara, Türkiye. TS EN, 2009. p. 196-1.
42. Colangelo F, Roviello G, Ricciotti L, Ferone C, Cio R. Preparation and characterization of new geopolymer-epoxy resin hybrid mortars. *Materials*. 2013;6(7):2989–3006. https://doi.org/10.3390/ma6072989.
43. https://atamankimya.com/sayfalar.asp?LanguageID=1&cid=3&id=10&id2=10780 (Accessed in: 02.02.2025).
44. ASTM Standards. Standard Test Method for Flow of Hydraulic Cement Mortar, West Conshohocken, United States. ASTM C, 2020. p. 1437–20.
45. Reeb C, Pierlot C, Davy C, Lambertin D. Incorporation of organic liquids into geopolymer materials - a review of processing, properties and applications. *Ceramics International*. 2021;47(6):7369–85. https://doi.org/10.1016/j.ceramint.2020.11.239.
46. Turkish Standard Institution. Methods of Test for Mortar for Masonry-Part 10: Determination of Dry Bulk Density of Hardened Mortar. Ankara, Türkiye. TS EN, 2001. p. 1015–10.
47. Turkish Standard Institution. Natural Building Stones-Methods of Inspection and Laboratory Testing. Ankara, Türkiye. TS, 2009. p. 699.
48. Turkish Standard Institution. Natural Stone Test Methods-Determination of Water Absorption Coefficient by Capillarity. Ankara, Türkiye. TS EN, 2000. p. 1925.
49. Turkish Standard Institution. Natural Stone Test Methods - Determination of Sound Speed Propagation. Ankara, Türkiye. TS EN, 2006. p. 14579.
50. Criado M, Fernandez-Jimenez A, Palomo A. Alkali activation of fly ash. Part III: Effect of curing conditions on reaction and its graphical description. *Fuel*. 2010;89(11):3185–92. https://doi.org/10.1016/j.fuel.2010.03.051.
51. Samantasinghar S, Singh S. Effects of curing environment on strength and microstructure of alkali-activated fly ash-slag binder. *Construction and Building Materials*. 2020;235:117481. https://doi.org/10.1016/j.conbuildmat.2019.117481.

52. Pacheco-Torgal F, Castro-Gomes J, Jalali S. Alkaliactivated binders: A review. Part 1. Historical background, terminology, reaction mechanisms and hydration products. *Construction and Building Materials*. 2008;22(7):1305–14. https://doi.org/10.1016/j.conbuildmat.2007.10.015.
53. El-Feky MS, Kohail M, El-Tair AM, Serag MI. Effect of microwave curing as compared with conventional regimes on the performance of alkali activated slag pastes. *Construction and Building Materials*. 2020;233:117268. https://doi.org/10.1016/j.conbuildmat.2019.117268.
54. Gültekin A. Effect of sealed water curing and fiber length on compressive strength and fracture energy of fly ash-based geopolymer mortars. *Journal of Sustainable Construction Materials and Technologies*. 2024;9(4):365–73. https://doi.org/10.47481/jscmt.1607851.
55. Catauro M, Papale F, Lamanna G, Bollino F. Geopolymer/PEG hybrid materials synthesis and investigation of the polymer influence on microstructure and mechanical behavior. *Materials Research*. 2015;18(4):698–705. https://doi.org/10.1590/1516-1439.342814.

Source details

Journal of Sustainable Construction Materials and Technologies

Open Access

Years currently covered by Scopus: from 2019 to 2025

Publisher: Kare Publishing

E-ISSN: 2458-973X

Subject area: Engineering: Building and Construction | Energy: General Energy | Engineering: Civil and Structural Engineering | Energy: Renewable Energy, Sustainability and the Environment

Source type: Journal

View all documents > | Set document alert | Save to source list

CiteScore 2024
1.6

SJR 2024
0.300

SNIP 2024
0.411

ISSN: 2458-973X

Volume 10, Issue 2 (2025)

PDF Effect of Reinforcement Thickness and Content on the Properties of Compressed Earth Blocks
Salah eddine Mokeddem, Abdelmadjid Hamouine, Rabia Abdeldjebar, and Atef Hamaidi

PDF Sustainable Modification of Stone Column Technique with Polyethylene Terephthalate (PET) Plastic for Strengthening the Expansive Clay
Ng Jun Shen and Muzamir Hasan

PDF Synergistic Effect of Alccofine as Partial Replacement of Cement and M-Sand as Sand Substitution in Concrete for the Assessment of Mechanical and Microstructural Properties
Yellinedi Madhavi, R.S. Ravichandran, J. Saravanan, and N. VenkataSairam Kumar

PDF Identification of Barriers and Drivers in the Adoption of Sustainable Construction Practices in the Turkish Construction Industry: Exploratory Factor Analysis
Tülay Çivici and Mustafa Serhan Ünlütürk

PDF Smart Traffic Management at Intersections
Gezim Hoxha, Piotr Gorzelanczyk, Rame Likaj, Shaban Thaqi, and Flori Cikaqi

PDF Rubber-Modified Self-Compacting Mortar: Evaluating Setting Time and Strength Development
Navvar Makansi, Süleyman Ipek, and Erhan Güneyisi

PDF Effect of Expanded Perlite and Exfoliated Vermiculite Aggregate Additives on Water Vapor Permeability Performance of Cement-Based Lightweight Mortars
Lütfullah Gündüz and Şevket Onur Kalkan

PDF NaOH Molarity Effect on Mechanical and Hydrochloric Acid Resistance of Geopolymer Mortar Based on Slag
Mahmoud Ziada and Zahraa Mohammed Kamil Al-Mayali

PDF Development of a Self-Cured Alkali-Activated Mortar
Kübra Ekiz Barış

PDF The Utilization of Basic Oxygen Furnace Slag as Fine Aggregates in Concrete: Physical, Mechanical, and Durability Properties
Hakan Ozkan



Editor-In-Chief



Orhan CANPOLAT, Ph.D.
Yildiz Technical University, Faculty of Civil Engineering, Department of Civil Engineering, Davutpaşa Campus 34210 Esenler, Istanbul, Türkiye
Contact: canpolat@yildiz.edu.tr (mailto:canpolat@yildiz.edu.tr)
ORCID: 0000-0003-2744-7876 (https://orcid.org/0000-0003-2744-7876)
Research Topics: Geopolymer Materials, Sustainable Construction Materials, Fiber Reinforced Concrete, Recycling and Reuse of Industrial Wastes, Durability and Performance Assessment

Editorial Board Members



Togay OZBAKKALOGLU, Ph.D., P.E.
College of Science and Engineering, Ingram School of Engineering, Texas State University, TX, United States
Contact: togay.oz@txstate.edu (mailto:togay.oz@txstate.edu)
ORCID: 0000-0003-3015-736X (https://orcid.org/0000-0003-3015-736X)
Scopus Author ID: 9741842600 (https://www.scopus.com/authid/detail.uri?authorId=9741842600)
Research Topics: Concrete materials, structural engineering, fiber-reinforced composites, earthquake engineering



Jamal KHATIB, Ph.D.
University of Wolverhampton, Wolverhampton, UK. / Beirut Arab University, Beirut, Lebanon
Contact: j.khatib@bau.edu.lb (mailto:j.khatib@bau.edu.lb)
ORCID: 0000-0002-4393-6728 (https://orcid.org/0000-0002-4393-6728)
Scopus Author ID: 6701635056 (https://www.scopus.com/authid/detail.uri?authorId=6701635056)
Research Topics: Sustainable construction materials, Construction & Building Technology, Environmental Sciences & Ecology



Xiaojian GAO, Ph.D.
Harbin Institute of Technology, School of Civil Engineering, China
Contact: gaoxj@hit.edu.cn (mailto:gaoxj@hit.edu.cn)
Scopus Author ID: 57215834431 (https://www.scopus.com/authid/detail.uri?authorId=57215834431)
Research Topics: Geotechnical engineering, soil mechanics, foundation engineering, underground construction



Muammer KOÇ, Ph.D.
Hamad bin Khalifa University, Sustainable Development, College of Science and Engineering (HBKU), Qatar
Contact: mkoc@hbku.edu.qa (mailto:mkoc@hbku.edu.qa)
ORCID: 0000-0001-6543-8116 (https://orcid.org/0000-0001-6543-8116)
Scopus Author ID: 57204468983 (https://www.scopus.com/authid/detail.uri?authorId=57204468983)
Research Topics: Sustainable manufacturing, renewable energy systems, circular economy, industrial engineering



Messaoud SAIDANI, Ph.D.
Associate Head of School, School of Energy, Construction and Environment, Coventry University, UK
Contact: cbx086@coventry.ac.uk (mailto:cbx086@coventry.ac.uk)
ORCID: 0000-0002-5861-676X (https://orcid.org/0000-0002-5861-676X)
Scopus Author ID: 6701603889 (https://www.scopus.com/authid/detail.uri?authorId=6701603889)
Research Topics: Structural engineering, finite element analysis, steel structures, sustainable construction



Mustafa ŞAHMARAN, Ph.D.
Hacettepe University, Engineering Faculty, Civil Engineering Department, Türkiye
Contact: sahmaran@hacettepe.edu.tr (mailto:sahmaran@hacettepe.edu.tr)
ORCID: 0000-0002-7549-096X (https://orcid.org/0000-0002-7549-096X)
Scopus Author ID: 21733527000 (https://www.scopus.com/authid/detail.uri?authorId=21733527000)
Research Topics: Self-healing concrete, durability of cement-based materials, nanomaterials in construction



Sudharshan N. RAMAN, Ph.D.
Monash University Malaysia, Civil Engineering Discipline, School of Engineering, Malaysia
Contact: sudharshan.raman@monash.edu (mailto:sudharshan.raman@monash.edu)
ORCID: 0000-0003-4149-0141 (https://orcid.org/0000-0003-4149-0141)
Scopus Author ID: 25637493900 (https://www.scopus.com/authid/detail.uri?authorId=25637493900)
Research Topics: Structural dynamics, earthquake engineering, sustainable construction materials



Rakesh KUMAR, Ph.D.
Chief Scientist and Professor, Academy of Scientific and Innovative Research; Head of Division, Rigid Pavement Division, New Delhi, India
Contact: rakeshcrri@nic.in (mailto:rakeshcrri@nic.in)
ORCID: 0000-0002-6723-4894 (https://orcid.org/0000-0002-6723-4894)
Scopus Author ID: 57306886500 (https://www.scopus.com/authid/detail.uri?authorId=57306886500)
Research Topics: Pavement engineering, concrete technology, materials characterization



Soofia Tahira Elias ÖZKAN, Ph.D.
Middle East Technical University, Department of Architecture, Türkiye
Contact: soofia@metu.edu.tr (mailto:soofia@metu.edu.tr)
Scopus Author ID: 15820509100 (https://www.scopus.com/authid/detail.uri?authorId=15820509100)
Research Topics: Recovery, Reuse, and Recycling of Building Materials, Sustainability in the Built Environment, Building Performance Simulations



Ali Naji ATTIYAH, Ph.D.
University of Kufa, Department of Civil Engineering, Iraq
Contact: alin.diebil@uokufa.edu.iq (mailto:alin.diebil@uokufa.edu.iq)
ORCID: 0000-0003-4615-3347 (https://orcid.org/0000-0003-4615-3347)
Research Topics: Structural analysis, Concrete technology, Seismic performance of buildings



Murat ATES, Ph.D.
Tekirdag Namık Kemal University, Department of Chemistry, Türkiye
Contact: mates@nku.edu.tr (mailto:mates@nku.edu.tr)
ORCID: 0000-0002-1806-0330 (https://orcid.org/0000-0002-1806-0330)
Scopus Author ID: 9735216100 (https://www.scopus.com/authid/detail.uri?authorId=9735216100)
Research Topics: Polymer chemistry, Nanomaterials, Advanced functional materials



Ghazi Al-KHATEEB, Ph.D.
University of Sharjah, College of Engineering, Department of Civil and Environmental Engineering, United Arab Emirates
Contact: galkhateeb@sharjah.ac.ae (mailto:galkhateeb@sharjah.ac.ae)
ORCID: 0000-0001-7917-1061 (https://orcid.org/0000-0001-7917-1061)
Scopus Author ID: 8442724600 (https://www.scopus.com/authid/detail.uri?authorId=8442724600)
Research Topics: Sustainable water resources management, Environmental engineering, Hydrological modeling, Wastewater treatment technologies



Huachao YANG, Ph.D.
College of Energy Engineering, Zhejiang University, Hangzhou, China
Contact: huachao@zju.edu.cn (mailto:huachao@zju.edu.cn)
ORCID: 0000-0002-9104-648X (https://orcid.org/0000-0002-9104-648X)
Research Topics: Renewable energy systems, Thermal energy storage, Heat transfer in construction materials, Energy-efficient building technologies



Sepanta NAIMI, Ph.D.
Altinbas University, Department of Civil Engineering, Türkiye
Contact: sepanta.naimi@altinbas.edu.tr (mailto:sepanta.naimi@altinbas.edu.tr)
ORCID: 0000-0001-8641-7090 (https://orcid.org/0000-0001-8641-7090)
Scopus Author ID: 54179598700 (https://www.scopus.com/authid/detail.uri?authorId=54179598700)
Research Topics: Structural engineering, Advanced concrete technology, Seismic resilience, Smart materials for infrastructure



Benchaa BENABED, Ph.D.
Université Amar Telidji Laghouat, Department of Civil Engineering, Algeria
Contact: b_benchaa@yahoo.fr (mailto:b_benchaa@yahoo.fr)
Scopus Author ID: 26325239700 (https://www.scopus.com/authid/detail.uri?authorId=26325239700)
Research Topics: High-performance concrete, Geopolymer composites, Recycled aggregate concrete, Mechanical properties and durability assessment



Siyu REN, Ph.D.
Nankai University, School of Economics, China
Contact: rensiyuking@126.com (mailto:rensiyuking@126.com)
ORCID: 0000-0002-0369-1519 (https://orcid.org/0000-0002-0369-1519)
Scopus Author ID: 57211439461 (https://www.scopus.com/authid/detail.uri?authorId=57211439461)
Research Topics: Sustainable economic development, Environmental economics, Resource management and circular economy, Socioeconomic impacts of construction practices



Muhammad Ashraf JAVID, Ph.D.
Faculty of Engineering, Sohar University, Oman
Contact: MJavid@su.edu.om (mailto:MJavid@su.edu.om)
ORCID: 0000-0003-3494-2891 (https://orcid.org/0000-0003-3494-2891)
Scopus Author ID: 56514248400 (https://www.scopus.com/authid/detail.uri?authorId=56514248400)
Research Topics: Transportation Demand Management (TDM) policies, Promotion of sustainable transport modes, Non-motorized transport facilities, Travel behavior modeling, Social-cognitive aspects of travel behavior, Shared mobility and shared economy, Traffic safety issues, Pavement materials characterization

We are currently inviting qualified researchers and academics to join the Editorial Board of our journal. If you are interested in contributing to the peer-review process and supporting the development of our publication, please submit your application through the form below.

Join the Board (https://forms.gle/N6JtjSdd7DHTc4yd8)